Journal of Alloys and Compounds 434–435 (2007) 729–733

Journal of
ALLOYS
AND COMPOUNDS

www.elsevier.com/locate/jallcom

Influence of impurities on the milling process of MgH_2

J.R. Ares [*], K.-F. Aguey-Zinsou, T. Klassen, R. Bormann

Institute for Materials Research, GKSS-Forschungszentrum, Max-Planck Str. 1, D-21502 Geesthacht, Germany

Abstract

Mechanical milling (MM) is an useful technique to improve the H-kinetics of magnesium hydride (MgH_2) by crystallite and particle size reduction. In the present work, we report the significant influence of impurities coming from the milling tools on magnesium H-sorption properties. We have observed that a high impurity level leads to powder agglomeration and subsequently, it prevents an efficient reduction of MgH_2 particle size. Therefore, a drawback in H-sorption properties is observed. Finally, a short outlook about the influence of impurities on desorption temperature of MgH_2 milled with different additives (metal-oxides) will be presented.

Keywords: Hydrogen absorbing materials; Mechanical alloying; Kinetics

1. Introduction

In the perspective of developing hydrogen-powered vehicles, on board H-storage is one of the main tasks to be fulfilled. At present, many materials have been considered to store hydrogen, but MgH_2 is very attractive because of its low cost and high storage capacity (7.6 wt%). Nevertheless, the practical use of MgH_2 for hydrogen storage is limited by its high thermodynamic stability and slow hydrogen kinetics [1]. It was recently found that the H-kinetics of MgH_2 could be improved by a particle size and crystallite size reduction obtained by mechanical milling (MM) [2]. Further improvement of H-kinetics' was achieved by milling MgH_2 with 3d transition metals (TM) and metal-oxides (M_xO_y) [3,4]. For example, Huot and co-workers [3] showed that MgH_2 milled with 5 wt% of Ti, V, Mn, Fe or Nb leads to excellent H-kinetics properties (H-desorption within few minutes at 250 °C). H-kinetics enhancement is mainly explained by catalytic effect of these metals on dissociation/recombination process of the H_2 molecule at the surface of MgH_2. On the other hand, Barkhordarian et al. [4] showed that MgH_2 milled with 1 mol% of different M_xO_y (TiO_2, V_2O_5, Mn_2O_3, Fe_3O_4, SiO_2) leads to similar improvement of H-kinetics properties with the main advantage of the lower price of the oxides compared to metals. Barkhordarian et al. claim that improvement of H-kinetics is related to the dissociation/recombination of hydrogen on the metal-oxides [4]. However, recent works [5–8] point out that oxides could help to refine MgH_2 powder during MM and thus, facilitate the formation of small particles of MgH_2. As a consequence, these particles should exhibit a fast H-sorption kinetics.

In the present work, we report, for the first time, the drastic influence of impurities from milling tools on MM process of MgH_2 and subsequently on H-kinetics properties. Structural, compositional, morphological as well as thermodynamic and kinetic properties have been investigated in two different milling environments: steel and ceramic vials. Influence of impurities on H-kinetics properties of MgH_2 milled with oxides (M_xO_y) will also be outlined. It will be concluded that the milling environment is an important parameter to consider for improving magnesium H-sorption properties.

2. Experimental

MgH_2 powder (95%, 50–150 μm) was purchased from Goldschmidt AG. The metal-oxides (Al_2O_3, TiO_2, SiO_2, Cr_2O_3 and Fe_2O_3) were purchased from Sigma–Aldrich.

A Frischt P5 planetary mill installed in a glove box flushed with Ar was used. MgH_2 was milled in ceramic and stainless steel vials using zirconium oxide balls (Ø10 mm, 3 g) and Cr-hardened steel balls (Ø10 mm, 4 g), respectively. The ball to powder weight ratio was 10:1. MgH_2 was also milled with 10 wt% of metal-oxides with the same conditions.

The elemental analysis of the sample was performed using an ICP-MS Perkin-Elmer Elan 6000. The structural characterization of the samples was carried out with a Bruker D8 Advance X-ray diffractometer using Cu Kα radiation. Diffraction patterns were analysed by the Rietveld method using the Fullprof software [9]. The sample morphology was characterised by SEM with a Zeiss DSM 962 apparatus.

---

[*] Corresponding author. Present address: Laboratorio de Materiales de Interés Enérgertico C-IV Dpto. Física de Materiales Facultad de Ciencias, Universidad Autónoma de Madrid, 28049, Madrid, Spain. Fax: +49 914978579.

E-mail address: joser.ares@uam.es (J.R. Ares).

0925-8388/$ – see front matter © 2006 Elsevier B.V. All rights reserved.
doi:10.1016/j.jallcom.2006.08.132

Calorimetric measurements were performed with a DSC 404 C Pegasus from Netzsch. The measurements were carried out under a flow of high purity Ar (50 mL min^{-1}) with a heating rate of 5 K min^{-1} from 25 to 500 °C. Hydrogen titration measurements were carried out with a Sievert apparatus designed by HERA Hydrogen Storage Systems. The measurements were performed at 300 °C at 1 MPa of hydrogen (99.999%) for absorption and 0.1 kPa for desorption.

3. Results and discussion

3.1. Microstructural properties of MgH_2^{steel} compared to MgH_2^{cera}

Fig. 1 shows the XRD patterns of MgH_2^{steel} (milled in steel vial), MgH_2^{cera} (milled in ceramic vial) milled for 200 h, and after the first cycle of hydrogen absorption and desorption. The phases were indexed to β-MgH_2, γ-MgH_2, MgO and Mg. As it was previously described [2], milling MgH_2 leads to a broadening of β-MgH_2 peaks due to the diminution of crystallite size and, the formation of a high pressure γ-MgH_2 phase (Table 1). Rietveld analyses of the XRD patterns of MgH_2^{steel} and MgH_2^{cera} show crystallite sizes of 9 ± 2 and 8 ± 1 nm, respectively. The unit cell volume of magnesium hydride was found to increase slightly (∼1%) during milling in steel as well ceramic vials. Finally, as concern the lattice strain at short milling times ($t < 200$ h), it increases in MgH_2^{steel} as well MgH_2^{cera} but at long milling times ($t > 200$ h) strain decreases in MgH_2^{steel} and it remains constant in MgH_2^{cera}. The first desorption and absorption of hydrogen (first cycle) at 300 °C leads to similar changes for both materials: (i) the metastable γ-MgH_2 phase transforms into β-MgH_2, and (ii) the crystallite size of β-MgH_2 increases significantly to values of 75 ± 10 nm. Moreover, the strain is released and the cell volume is reduced to the initial value. Therefore, MgH_2^{steel} and MgH_2^{cera} exhibit similar structures and microstructures during H-absorption/desorption measurements.

Fig. 2a and b show the measurements of the particle morphology by BSE. The initial MgH_2 particle size (40 ± 20 μm) is reduced to smaller sizes at short milling times (<200 h). At long milling times (>200 h), the small particles tend to agglomerate. Agglomeration is much more pronounced for MgH_2^{steel} than for MgH_2^{cera} as Fig. 2a and b show. We also have observed that annealing does not change this particle distribution.

3.2. Thermal stability and H-sorption properties of MgH_2^{steel} compared to MgH_2^{cera}

Fig. 3a shows the influence of milling time on decomposition temperature (T_d) of MgH_2. In the case of MgH_2^{steel}, T_d decreases from 414 ± 5 to 355 ± 4 °C after 20 h of milling.

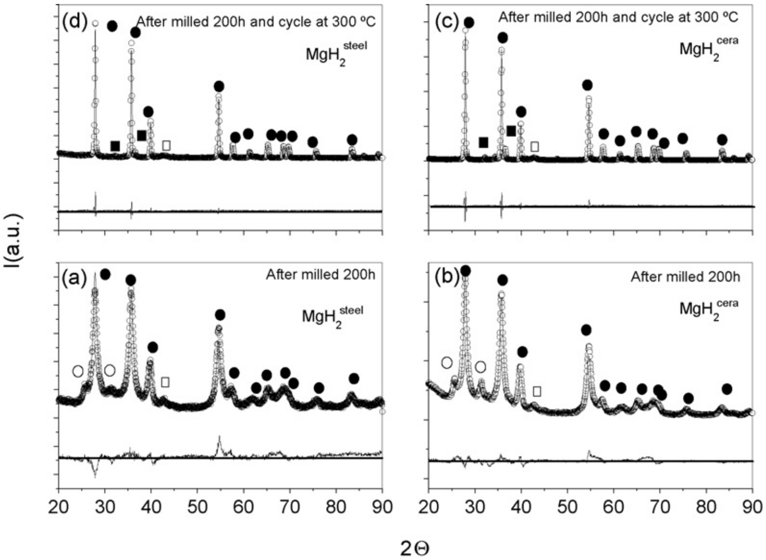

Fig. 1. XRD patterns of (a) MgH_2^{steel}, (b) MgH_2^{cera} milled 200 h and, after the initial cycle of hydrogen desorption and absorption at 300 °C of (c) MgH_2^{steel} and (d) MgH_2^{cera}. Continuous line is the Rietveld fit ($R_{wp} < 11\%$). Symbols corresponding to following phases: MgO (□), β-MgH_2 (●), γ-MgH_2 (○), Mg (■).

Table 1
Microstructural parameters of β-MgH_2 phase of MgH_2^{steel} and MgH_2^{cera} milled different times and after 1 cycle

Milling time (h)	MgH_2^{steel}			MgH_2^{cera}		
	D_v (nm)	ε (%)	V (Å^3)	D_v (nm)	ε (%)	V (Å^3)
0	400 ± 50	0.005 ± 0.001	61.59 ± 0.01	400 ± 50	0.005 ± 0.001	61.59 ± 0.01
20	12 ± 2	0.15 ± 0.01	61.57 ± 0.02	10 ± 1	0.54 ± 0.05	61.64 ± 0.02
200	9 ± 2	0.4 ± 0.1	61.94 ± 0.01	9 ± 1	0.52 ± 0.05	61.79 ± 0.04
700	8 ± 2	0.15 ± 0.02	62.55 ± 0.02	8 ± 1	0.5 ± 0.05	61.85 ± 0.02
1 cycle	70 ± 6	0.01 ± 0.01	61.69 ± 0.01	77 ± 5	0.07 ± 0.04	61.65 ± 0.03

D_v is the crystallite size, ε the lattice strain and V is the unit cell volume of MgH_2 phase.

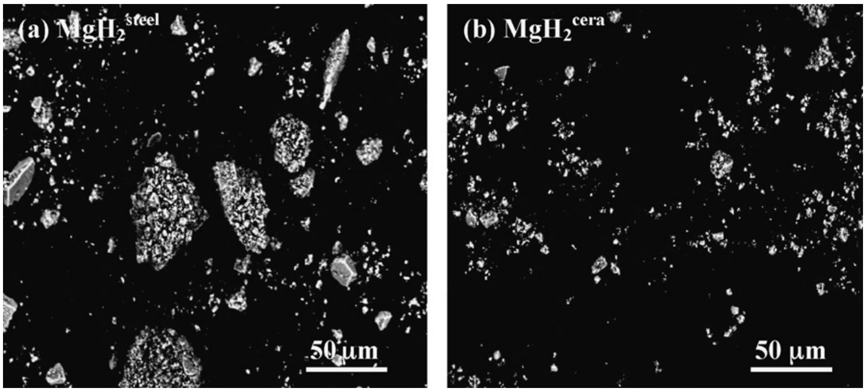

Fig. 2. Backscattered secondary electron images (BSE) of (a) MgH_2^{steel} and (b) MgH_2^{cera} milled 200 h.

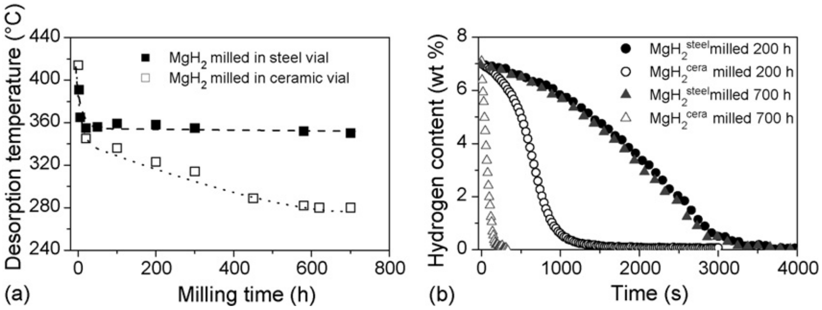

Fig. 3. (a) Influence of milling time on decomposition temperature of MgH_2^{steel} and MgH_2^{cera} obtained by DSC at 5 K/min and (b) desorption H-kinetics of MgH_2^{steel} and MgH_2^{cera} for different milling times at 300 °C.

Further milling does not allow any additional improvement. However, at long milling times, T_d of MgH_2^{cera} decreases. Then, for example, MgH_2^{cera} milled 700 h decomposes at $T_d = 280 \pm 4\,°C$ while MgH_2^{steel} decomposes at $T_d = 350\,°C$. This behaviour is also observed by the desorption H-kinetics at 300 °C of MgH_2^{steel} and MgH_2^{cera}. For example, Fig. 3b shows that, whereas MgH_2^{steel} milled for 200 h is completely desorbed in ∼4000 s, MgH_2^{cera} is desorbed in ∼1500 s. At longer milling time (700 h), the desorption kinetics of MgH_2^{cera} is further improved (∼200 s) and it shows similar desorption rates than those obtained when MgH_2 is milled with metal-oxides [4].

MgH_2^{steel} and MgH_2^{cera} exhibit similar microstructure but different morphology. Therefore, the different particle size distribution should be considered to explain the different H-kinetics. In fact, it is well known that MM is a complex mechanism that involves processes of particle cracking (at shorter milling times) and processes of agglomeration or cold-welding (at longer milling times). Therefore, the physical properties of the different materials and environments during this process should have a drastic influence on the milling mechanism and, subsequently, on H-properties of MgH_2. In fact, the improvement on H-kinetics due to particle size reduction of MgH_2 milled with some additives such as graphite (lubricant properties) or SiC (high hardness) has been reported recently [10].

In our case, ICP measurements reveal a different concentration and kind of impurities for MgH_2^{steel} and MgH_2^{cera} as Fig. 4 shows. Whereas in MgH_2^{steel} the concentration of iron impurities increases with the milling time up to 4 wt% after 700 h of milling, MgH_2^{cera} exhibits much less amount of impurities. After 700 h of milling, only 0.6 wt% of Zr (related to the vial tools) is detected. In the first case, the high amounts of Fe impurities seem to facilitate the particle agglomeration and cold-welding, thus they prevent a further particle size reduction as Fig. 2a shows. Moreover, at long milling times (>200 h), the lattice strain of MgH_2^{steel} decreases suggesting that milling energy is dissipated within the larger agglomerates and milling process is less efficient. The lower agglomeration of MgH_2 particles milled in ceramic vial compared to those milled in steel vial

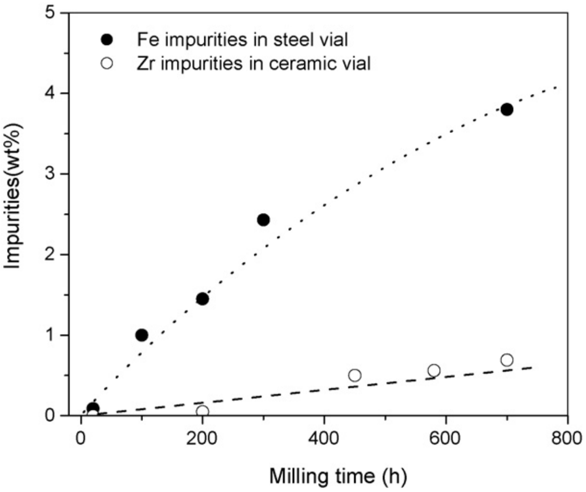

Fig. 4. Influence of milling time on impurities concentration of MgH_2^{steel} and MgH_2^{cera} obtained by ICP measurements.

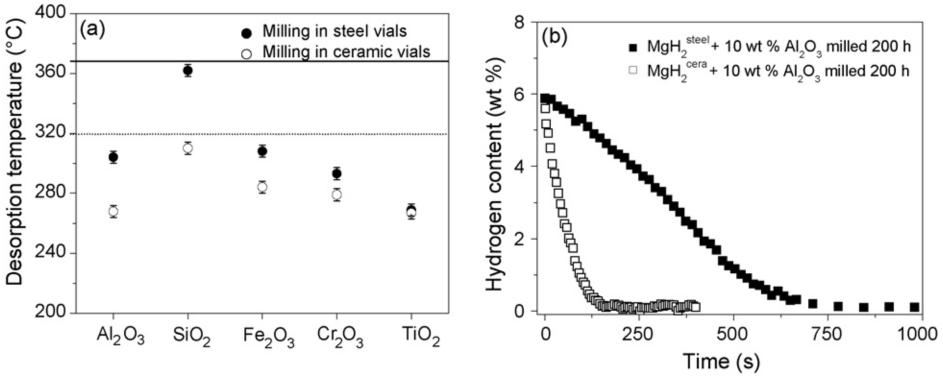

Fig. 5. (a) Influence of different metal-oxides on the decomposition temperature of MgH_2^{steel} and MgH_2^{cera} milled for 200 h. The decomposition temperatures materials have been obtained by DSC. Straight and dashed lines correspond to decomposition temperature of MgH_2^{steel} and MgH_2^{cera} milled for 200 h, respectively, and (b) H-desorption kinetics of MgH_2^{steel} and MgH_2^{cera} milled with Al_2O_3 for 200 h.

leads to faster H-kinetics as well as the fast H-sorption kinetics observed in MgH_2 milled very long times in ceramic vial.

3.3. Thermal stability and H-sorption properties of MgH_2^{steel} compared to MgH_2^{cera} milled with different oxides

It is known that MgH_2 milled with oxides exhibits a lower T_d than that of MgH_2 milled for the same duration [4]. At present, this effect is explained by two reasons: the catalytic effect of the metal-oxides [4] and their ability to reduce particle size [5,8]. With regard to the particle size, besides of the influence of mechanical properties of the oxides (hardness) on particle size reduction, the particle agglomeration in MgH_2 caused by MM is a phenomena that prevents also a further reduction on the particle size and, therefore, an improvement on H-kinetics. Particle agglomeration in MgH_2 is related to electrostatic forces among particles due to the ionic character of MgH_2 [11] Hence, process of particle size reduction could be improved by using polar-oxides to avoid agglomeration of MgH_2. These oxides exhibit two effects: (i) they prevent agglomeration of MgH_2 particles and (ii) they may generate MgH_2 and metal-oxide interfaces which may improve hydrogen kinetics [12]. Fig. 5a shows the desorption temperatures of MgH_2 milled for 200 h with different oxides in a ceramic vial (Zr impurities <1wt%). It is observed that by using oxides with a strong ionic character (polar-oxides) such as Al_2O_3, TiO_2, ..., the desorption temperature of MgH_2 decreases as compared to that obtained in oxides with a weak ionic character (near covalent bond) such as SiO_2. Moreover, MgH_2 milled with oxides such as MgO [6] (it exhibits higher ionic character than TiO_2, Al_2O_3 or Nb_2O_5), H-kinetics is radically improved by particle size reduction. Finally, mechanical properties such as hardness, ductility, etc. of the oxides seem to have great influence on H-kinetic of MgH_2. We have observed that among oxides with similar ionic character, i.e. Al_2O_3 versus TiO_2, the hardest oxide enhances the process of particle size reduction and, therefore H-kinetics of MgH_2 is improved.

In this context, impurities from the milling tools also show an influence on hydrogenation properties of MgH_2 milled with metal-oxides. Fig. 5a shows that MgH_2 milled in a steel vial leads to a higher T_d than when milled in ceramic vial (without impurities). As detailed in Fig. 5b, desorption kinetics of MgH_2 milled with Al_2O_3 at 300 °C is six times faster when it is milled in ceramic vials than in steel vials. The quantity of Fe impurities (2–10 wt%) coming from steel vial depends on additive used. It is remarkable that hardest oxides (Al_2O_3) do not lead to a higher amount of impurities suggesting that much more complicated process could occur during milling such as mechanical alloying among oxides and impurities, etc. Then, impurities may have a great influence on the surface properties of the MgH_2 particles and subsequently on the process of particle reduction. In order to understand the improvement on H-kinetics caused by this additive it is necessary to take into account the influence of such impurities. Further investigations are currently in progress to understand the influence of impurities (hardness, surface potential) on the milling process and, subsequently on particle size reduction that occurs during milling.

4. Conclusion

MgH_2 with and without additives (M_xO_y) were milled using ceramic and steel milling tools. MgH_2 milled in ceramic vial exhibits a faster H-kinetics than this milled in steel vial. Therefore, H-kinetics of MgH_2 is significantly influenced by the contamination resulting from the milling tools. When steel vials are used, the contamination of the powder with Fe impurities leads to particle agglomeration and cold-welding, thus preventing further decrease of MgH_2 particle size. On the other hand, oxides may help to avoid agglomeration due to their polar character. They show a positive effect on H-kinetics of MgH_2. Finally, impurities from the milling tools show a negative influence on the H-kinetics of MgH_2.

Acknowledgement

Financial support by the E.U. (contract number: HPRN-CT-2002-00208) is gratefully acknowledged.

References

[1] B. Bogdanovic, A. Ritter, B. Splichthoft, Angew. Chem. 29 (1990) 223–234.

[2] J. Huot, G. Liang, S. Bobet, A. Van Neste, R. Schulz, J. Alloys Compd. 295 (1999) 495–500.

[3] G. Liang, J. Huot, S. Boily, A. Van Neste, R. Schulz, J. Alloys Compd. 292 (1999) 247–252.

[4] G. Barkhordarian, T. Klassen, R. Bormann, J. Alloys Compd. 364 (2004) 242–246.

[5] F.K. Aguey-Zinsou, J.R. Ares, T. Klassen, R. Bormann, unpublished.

[6] F.-K. Aguey-Zinsou, J.R. Ares, T. Klassen, R. Bormann, Mater. Res. Bull. 41 (6) (2006) 1118–1126.

[7] M. Song, Ik. Kwon, S. Kwon, C. Park, H.R. Park, J. Bae, J. Alloys Compd. 396 (2005) 264–268.

[8] D. Fátay, Á. Révész, T. Spassov, J. Alloys Compd. 399 (2005) 237–241.

[9] J. Rodriguez-Carvajal, Phys. B 192 (1993) 55–69.

[10] M. Güvendiren, E. Bayböru, T. Öztürk, Int. J. Hydrogen Energy 29 (2004) 491–496.

[11] H.J. Fecht, Nano Mater. 6 (1995) 33–42.

[12] M. Porcu, A.K. Petford-Long, J. M. Sykes, Unpublished.